

chap. 11.3, pp. 480-497,
in Environmental and Space Electromagnetics,
H. Kikuchi (ed.), Springer Verlag, 1991.

WL-EMP-SSN-314

Sensor and Simulation Notes

Note 314

18 November 1988

Some Features of Waveguide/Horn Design

Carl E. Baum

Air Force Weapons Laboratory

Abstract

In transitioning a sinusoidal electromagnetic wave from source to radiating antenna a conducting waveguide operating in the lowest order H mode is often used. This waveguide can be optimized for its power handling capabilities. As a common rectangular waveguide the $H_{1,0}$ mode has geometric properties which allow E-plane subdivision into some number of rectangular guides. This in turn allows convenient division or recombination of electromagnetic waves. This concept is extended to pyramidal horns which can launch the waves from one or more waveguides. The E-plane subdivision can be used for designing a metallic grating which allows passage of the wave while mechanically supporting a dielectric sheet separating vacuum from gas regions.

sinusoidal electromagnetic waves, conductors

CLEARED FOR PUBLIC RELEASE

AFWL/PA 89-51

2/16/89

I. Introduction

This paper considers some of the aspects of waveguides for transmitting electromagnetic waves from one or more sources to one or more horns for constructing a radiating electromagnetic wave at the aperture plane or array surface (for an array of horns). Such a waveguide/horn system can be an integral part of a source/antenna system such as discussed in [1].

Beginning with a review of the modes in a perfectly conducting waveguide the power handling capability is considered. Constraining operation to the lowest order mode (an H mode) a dimensionless efficiency factor is defined. Paying special attention to the usual rectangular waveguide the various parameters are discussed for the $H_{1,0}$ mode.

Concerning the lowest order H mode of a perfectly conducting waveguide it is possible to place perfectly conducting sheets which do not interfere with this mode. For the rectangular waveguide these sheets are planes. These can be used to divide the $H_{1,0}$ mode of one waveguide into the same mode of several rectangular waveguides but with a smaller height-to-width ratio. Alternatively the same technique can combine the waves in several waveguides (as from several sources) into one waveguide provided that the amplitudes and phases of the several waves are properly matched into the single waveguide.

Expanding the waveguide into a horn (a conical waveguide) the electric field can be reduced to go from a medium of high dielectric strength (such as high vacuum) to a lower strength medium (such as air or some other gas). Noting the electromagnetic field distribution in the lowest H mode as in the waveguide similar conducting sheets can be placed in non-interfering positions in the horn. One use of these is as a metal grating to support a dielectric pressure barrier between high vacuum and some gas (such as air or a special high-dielectric-strength gas). Expanding this special grating back into the throat of the horn the conducting sheets can be modified via corrugation to give a slow-wave character to the waves passing between the sheets and thereby form a lens to modify the phase distribution on the horn aperture.

II. Modes in Closed Perfectly Conducting Waveguides

The basic theory of closed conducting waveguides is now summarized following [3]. As in Figure 2.1 we have a rectangular coordinate system

$$\vec{r} = (x, y, z) \quad (2.1)$$

where the waveguide cross section is independent of z . Designate the cross-section surface (on the $z = 0$ plane) as S with outer boundary C oriented with tangent vector \vec{i}_C . The unit normal to S

$$\vec{i}_S = \vec{i}_z \quad (2.2)$$

with $\vec{i}_C \times \vec{i}_z$ as the outward unit normal on C .

The modes come in precisely two kinds (no hybrid modes as on an open dielectric waveguide). For the H (or TE) modes we have a real valued scalar function $\psi_{h,\beta}$ satisfying a two-dimensional Helmholtz equation

$$\begin{aligned} [\nabla_t^2 + k_{h,\beta}^2] \psi_{h,\beta}(x,y) &= 0 \\ \nabla_t^2 &= \frac{\partial^2}{\partial x^2} + \frac{\partial^2}{\partial y^2} \end{aligned} \quad (2.3)$$

$$[\vec{i}_C \times \vec{i}_z] \cdot \nabla_t \psi_{h,\beta}(x,y) = 0 \quad \text{on } C$$

$$\nabla_t = \vec{i}_x \frac{\partial}{\partial x} + \vec{i}_y \frac{\partial}{\partial y}$$

$\beta \equiv$ mode index set

The $k_{h,\beta}$ are real-valued cutoff wave numbers [2]. The fields take the form

$$H_{z,h,\beta} = k_{h,\beta}^2 e^{\pm \gamma_{z,h,\beta} z} \psi_{h,\beta}(x,y) \quad (\text{hence an H mode})$$

$$\vec{H}_{t,h,\beta} = \pm \gamma_{z,h,\beta} e^{\pm \gamma_{z,h,\beta} z} \nabla_t \psi_{h,\beta}(x,y) \quad (2.4)$$

$$\vec{E}_{t,h,\beta} = \pm \gamma_{z,h,\beta} \vec{i}_z \times \vec{H}_{t,h,\beta} = s \mu_0 e^{\pm \gamma_{z,h,\beta} z} \vec{i}_z \times \nabla_t \psi_{h,\beta}(x,y)$$

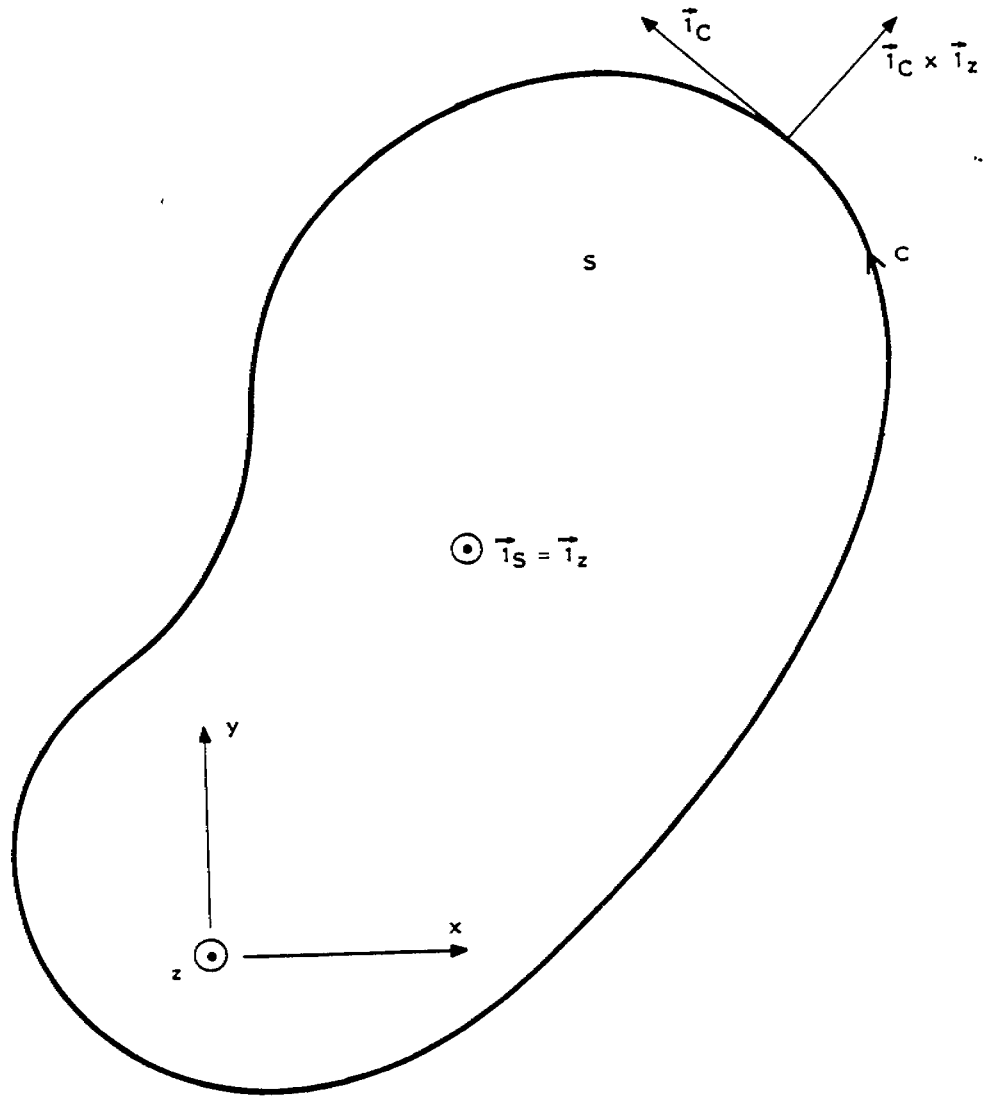


Figure 2.1. Cross Section of Closed Perfectly Conducting Waveguide

Here a subscript "t" indicates the transverse part. Various other parameters are

$$\begin{aligned}
 \gamma &= \frac{s}{c} \text{ (free-space propagation constant)} \\
 Z_0 &= \sqrt{\frac{\mu_0}{\epsilon_0}} = 377 \Omega \text{ (free-space impedance)} \\
 c &= \frac{1}{\sqrt{\mu_0 \epsilon_0}} = 3 \times 10^8 \frac{\text{m}}{\text{s}} \text{ (free-space propagation speed)} \\
 \gamma^2 &= \gamma_{z_{h,\beta}}^2 + \gamma_{h,\beta}^2 = \gamma_{z_{h,\beta}}^2 - k_{h,\beta}^2 \\
 Z_{h,\beta} &= \frac{s \mu_0}{\gamma_{z_{h,\beta}}} = \frac{\gamma}{\gamma_{z_{h,\beta}}} Z_0 \text{ (modal impedance)}
 \end{aligned} \tag{2.5}$$

In terms of the $j\omega$ axis (ω real) we have

$$\begin{aligned}
 \gamma &= jk, \quad s = j\omega, \quad k = \frac{\omega}{c} \\
 \gamma_{z_{h,\beta}} &= jk_{z_{h,\beta}} \text{ (guide propagation constant)} \\
 \zeta_{h,\beta} &= \left[1 - \left(\frac{k_{h,\beta}}{k} \right)^2 \right]^{1/2} < 1 \text{ for } 0 < \frac{k_{h,\beta}}{k} < 1 \\
 Z_{h,\beta} &= \zeta_{h,\beta}^{-1} Z_0 \\
 k_{z_{h,\beta}} &= k \zeta_{h,\beta} \text{ (guide wave number)} \\
 f_{h,\beta} &= \frac{1}{2\pi} \omega_{h,\beta} = \frac{c}{\gamma_{h,\beta}} \text{ (cutoff frequency)} \\
 \lambda_{h,\beta} &= \frac{2\pi}{k_{h,\beta}} \text{ (cutoff wavelength)}
 \end{aligned} \tag{2.6}$$

For the E (or TM) modes we have a real valued scalar function $\psi_{e,\beta}$ satisfying a two-dimensional Helmholtz equation

$$\begin{aligned} [\nabla_t^2 + k_{e,\beta}^2] \psi_{e,\beta}(x,y) &= 0 \\ \psi_{e,\beta}(x,y) &= 0 \text{ on } C \end{aligned} \quad (2.7)$$

Again the $k_{e,\beta}$ are real-valued cutoff wave numbers [2]. The fields take the form

$$\begin{aligned} E_{z_{e,\beta}} &= k_{e,\beta}^2 e^{\pm \gamma_{z_{e,\beta}} z} \psi_{e,\beta}(x,y) \quad (\text{hence an E mode}) \\ \vec{E}_{t_{e,\beta}} &= \pm \gamma_{z_{e,\beta}} e^{\pm \gamma_{z_{e,\beta}} z} \nabla_t \psi_{e,\beta}(x,y) \\ \vec{H}_{t_{e,\beta}} &= \mp Y_{e,\beta} \hat{i}_z \times \vec{E}_{t_{e,\beta}} = -s \epsilon_0 e^{\pm \gamma_{z_{e,\beta}} z} \hat{i}_z \times \nabla_t \psi_{e,\beta}(x,y) \end{aligned} \quad (2.8)$$

Various other parameters are

$$\begin{aligned} \gamma^2 &= \gamma_{z_{e,\beta}}^2 + \gamma_{e,\beta}^2 = \gamma_{z_{e,\beta}}^2 - k_{e,\beta}^2 \\ Y_{e,\beta} &= \frac{s \epsilon_0}{\gamma_{z_{e,\beta}}} = \frac{\gamma}{\gamma_{z_{e,\beta}}} Y_0 \quad (\text{modal admittance}) \\ Y_0 &= Z_0^{-1} \quad (\text{free-space admittance}) \end{aligned} \quad (2.9)$$

In terms of the $j\omega$ axis we have

$$\gamma_{z_{e,\beta}} = jk_{z_{e,\beta}} \quad (\text{guide propagation constant})$$

$$\zeta_{e,\beta} = \left[1 - \left(\frac{k_{e,\beta}}{k} \right)^2 \right]^{1/2} < 1 \quad \text{for} \quad 0 < \frac{k_{e,\beta}}{k} < 1$$

$$Y_{e,\beta} = \zeta_{e,\beta}^{-1} Y_0$$

(2.10)

$$k_{z_{e,\beta}} = k \zeta_{e,\beta} \quad (\text{guide wave number})$$

$$f_{e,\beta} = \frac{1}{2\pi} \omega_{e,\beta} = \frac{c}{\lambda_{e,\beta}} \quad (\text{cutoff frequency})$$

$$\lambda_{e,\beta} = \frac{2\pi}{k_{e,\beta}} \quad (\text{cutoff wavelength})$$

As shown in [3] there are a set of mode orthogonality conditions which we summarize as

$$\int_S \psi_{v_1} \psi_{v_2} dS = 0$$

$$\int_S \left[\nabla_t \psi_{v_1} \right] \cdot \left[\nabla_t \psi_{v_2} \right] dS = 0$$

(2.11)

$$\int_S \left[\hat{i}_z \times \nabla_t \psi_{v_1} \right] \cdot \left[\hat{i}_z \times \nabla_t \psi_{v_2} \right] dS = 0$$

$$\int_S \left[\hat{i}_z \times \nabla_t \psi_{v_1} \right] \cdot \left[\nabla_t \psi_{v_2} \right] dS = 0$$

$$v = \begin{pmatrix} e \\ h \end{pmatrix}, \beta \equiv \text{index set designating any mode (E or H)}$$

These results apply for any combination of modes with the sufficient condition

$$k_{v_1} \neq k_{v_2} \quad \text{for} \quad v_1 \neq v_2 \quad (2.12)$$

Now while this is a sufficient condition there are many cases of waveguides involving symmetrical cross sections where the degeneracy of equal cutoff wave numbers for different v_1 and v_2 does not lead to exceptions to (2.11). So it is known that (2.12) is often not necessary.

III. Power in Waveguide Modes

The peak power in a waveguide is

$$\begin{aligned}
 P &= \int_S [\vec{E} \times \vec{H}^*] \cdot \vec{i}_z \, dS \\
 &= 2 P_{\text{avg}}
 \end{aligned} \tag{3.1}$$

$P_{\text{avg}} \equiv$ average power

where we have chosen the mode to be propagating in the +z direction and set $z=0$ for the integration. Also with $s=j\omega$ we have assumed that k is greater than the cutoff wave number. For H modes only the transverse components contribute and (2.4) gives

$$\begin{aligned}
 P_{h,\beta} &= -k^2 Z_0 \zeta_{h,\beta} \int_S \left\{ [\vec{i}_z \times \nabla_t \psi_{h,\beta}(x,y)] \times [\nabla_t \psi_{h,\beta}(x,y)] \right\} \cdot \vec{i}_z \, dS \\
 &= k^2 Z_0 \zeta_{h,\beta} \int_S |\nabla_t \psi_{h,\beta}(x,y)|^2 \, dS
 \end{aligned} \tag{3.2}$$

Similarly for E modes we have from (2.8)

$$\begin{aligned}
 P_{e,\beta} &= k^2 Y_0 \zeta_{e,\beta} \int_S \left\{ [\nabla_t \psi_{e,\beta}(x,y)] \times [\vec{i}_z \times \nabla_t \psi_{e,\beta}(x,y)] \right\} \cdot \vec{i}_z \, dS \\
 &= k^2 Y_0 \zeta_{e,\beta} \int_S |\nabla_t \psi_{e,\beta}(x,y)|^2 \, dS
 \end{aligned} \tag{3.3}$$

Alternate expressions can be found using the relation valid for both H and E modes [3].

$$\begin{aligned}
 &\int_S |\nabla_t \psi_v(x,y)|^2 \, dS \\
 &= k_v^2 \int_S \psi_v^2(x,y) \, dS
 \end{aligned} \tag{3.4}$$

IV. Power Handling Capability of Waveguide in Lowest Order H Mode

Now let us consider that the waveguide is being operated in its lowest order mode, an H mode. Let the subscript "0" be used to designate parameters for this mode. Now we have $k > k_0$ for this mode to propagate. As frequency is increased other modes can also propagate. Let the subscript "1" be used to designate frequency/wavelength parameters for the next mode (or modes if more than one have the same cutoff frequency). Then to operate in the lowest order mode we have

$$\begin{aligned}k_0 &< k < k_1 \\f_0 &< f < f_1 \\ \lambda_0 &> \lambda > \lambda_1\end{aligned}\tag{4.1}$$

Let us define a relative bandwidth for the lowest order mode as

$$\eta_f \equiv \frac{f_1}{f_0} = \frac{k_1}{k_0} = \frac{\lambda_0}{\lambda_1}\tag{4.2}$$

One measure of waveguide optimization is the maximization of this relative bandwidth, such as for communications purposes. It is known that the lowest order mode is an H mode as is the next mode, so only H modes need to be considered to determine both k_0 and k_1 [2].

From (3.2) the power (peak) in the lowest order H mode is

$$\begin{aligned}P_0 &= k^2 Z_0 \zeta_0 \int_S |\nabla_t \psi_0(x,y)|^2 dS \\ \zeta_0 &= \left[1 - \left(\frac{k_0}{k} \right)^2 \right]^{1/2}\end{aligned}\tag{4.3}$$

From (2.4) we have the maximum electric field magnitude on S as

$$E_0 \equiv \max_S \omega \mu_0 |\nabla_t \psi_0(x,y)|\tag{4.4}$$

Defining a normalizing power density as

$$p_o \equiv \frac{E_o^2}{Z_o} \quad (4.5)$$

The power can be normalized to give an effective guide area as

$$A_o \equiv \frac{P_o}{p_o} = \left[\max_S |\nabla_t \psi_o(x,y)| \right]^{-2} \zeta_o \int_S |\nabla_t \psi_o(x,y)|^2 dS \quad (4.6)$$

For some specified peak electric field E_o (related to breakdown) then $A_o p_o$ gives the power handling capability of the guide (peak, not average). In maximizing A_o note the geometric part involving ψ_o . There is also a frequency part contained in ζ_o . For a given waveguide size and shape we can maximize ζ_o subject to (4.1). Taking the limit as $k \rightarrow k_1$ we define

$$\zeta_1 \equiv \left[1 - \left(\frac{k_o}{k_1} \right)^2 \right]^{\frac{1}{2}} = \left[1 - \eta_f^{-2} \right]^{\frac{1}{2}} \quad (4.7)$$

$$A_1 \equiv \left[\max_S |\nabla_t \psi_o(x,y)| \right]^{-2} \zeta_1 \int_S |\nabla_t \psi_o(x,y)|^2 dS$$

Now A_1 is only a function of the size and shape of the waveguide via ψ_o and ζ_1 .

We can define as associated effective length which we wish to maximize as

$$l_1 \equiv A_1^{\frac{1}{2}} \quad (4.8)$$

Noting a frequency/distance inverse scaling define a dimensionless parameter as

$$\eta_1 \equiv \frac{f_1 l_1}{c} = \frac{l_1}{\lambda_1} \quad (4.9)$$

For a given desired operating frequency f_1 we wish to maximize l_1 to maximize the power handling capability of the guide in its lowest mode.

Combining the above results gives

$$\begin{aligned}
 \eta_1 &= \frac{1}{\lambda_1} \left[\max_S |\nabla_t \psi_0(x,y)| \right]^{-1} \left\{ \zeta_1 \int_S |\nabla_t \psi_0(x,y)|^2 dS \right\}^{1/2} \\
 &= \frac{2\pi}{\lambda_1 \lambda_0} \left[\max_S |\nabla_t \psi_0(x,y)| \right]^{-1} \left\{ \zeta_1 \int_S \psi_0^2(x,y) dS \right\}^{1/2} \\
 &= \frac{\eta_f}{\lambda_0} \left[\max_S |\nabla_t \psi_0(x,y)| \right]^{-1} \left\{ \zeta_1 \int_S |\nabla_t \psi_0(x,y)|^2 dS \right\}^{1/2} \\
 &= \frac{2\pi \eta_f}{\lambda_0^2} \left[\max_S |\nabla_t \psi_0(x,y)| \right]^{-1} \left\{ \zeta_1 \int_S \psi_0^2(x,y) dS \right\}^{1/2}
 \end{aligned} \tag{4.10}$$

as several alternate forms of this dimensionless efficiency factor. Maximizing η_1 optimizes the shape of the waveguide cross section for maximum power handling.

In some cases the electric field E_0 for breakdown may be more important on C than throughout S . For example, under sufficiently high vacuum conditions one is concerned about field emission from the waveguide walls. Then one can replace

$$\max_S |\nabla_t \psi_0(x,y)| \rightarrow \max_C |\nabla_t \psi_0(x,y)| \tag{4.11}$$

in the previous formulae. To distinguish this case η_1 might be replaced by η_1' .

V. Rectangular Waveguide

As a common example consider the widely used rectangular waveguide as exhibited in Figure 5.1. Let the guide be described by

$$(x,y) \in S \quad \text{for} \quad \begin{cases} 0 \leq x \leq a \\ 0 \leq y \leq b \end{cases}$$
$$0 < b \leq a \quad (5.1)$$

Following [3] the H modes have

$$\psi_{h,n,m} = \cos\left(\frac{n\pi x}{a}\right) \cos\left(\frac{m\pi y}{b}\right) \quad (5.2)$$

$$n = 0, 1, 2, 3, \dots$$

$$m = 0, 1, 2, 3, \dots$$

but not both $n = 0$ and $m = 0$

$$\lambda_{h,n,m} = \frac{2\pi}{k_{h,n,m}} = 2\left[\left(\frac{n}{a}\right)^2 + \left(\frac{m}{b}\right)^2\right]^{-1/2}$$

The lowest order H mode is the $H_{1,0}$ mode for which

$$\lambda_{h,1,0} = 2a$$

$$\psi_{h,1,0} = \cos\left(\frac{\pi x}{a}\right) \quad (5.3)$$

$$\nabla_t \psi_{h,1,0} = -\frac{\pi}{a} \sin\left(\frac{\pi x}{a}\right) \hat{i}_x$$

Then \vec{H}_t has only an x component and \vec{E}_t has only a y component, both with the sine variation as above going to zero on the side walls.

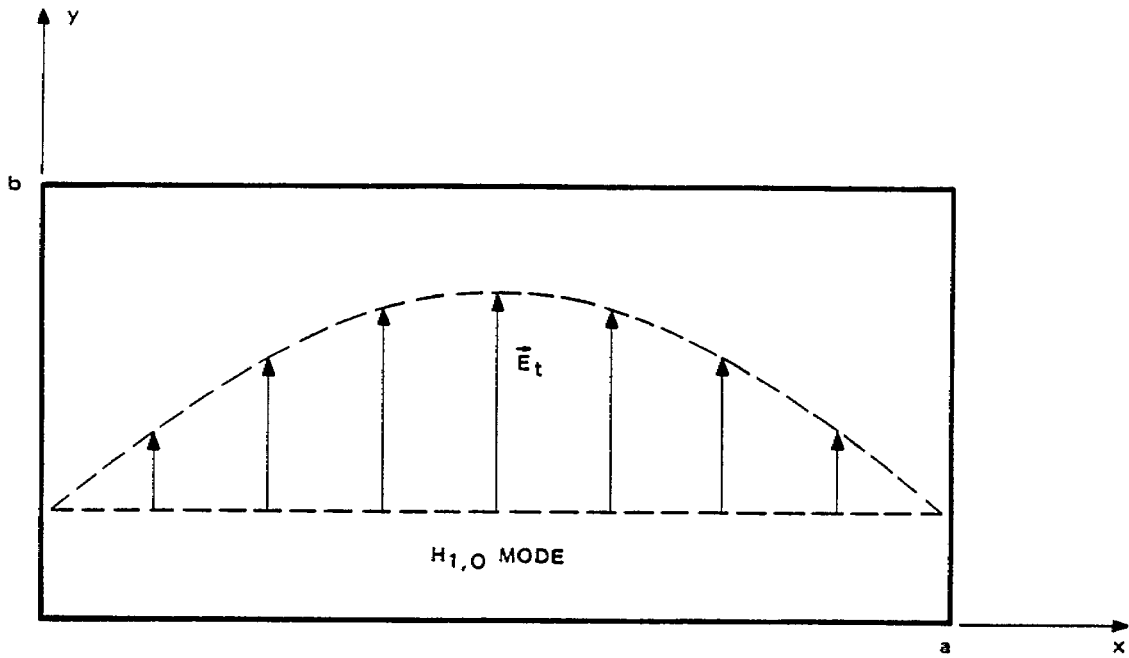


Figure 5-1. Rectangular Waveguide Cross Section and Lowest Order H Mode

Similarly the E modes have

$$\begin{aligned}\psi_{e,n,m} &= \sin\left(\frac{\pi x}{a}\right) \sin\left(\frac{\pi x}{b}\right) \\ n &= 1, 2, 3, \dots \\ m &= 1, 2, 3, \dots \\ \lambda_{e,n,m} &= \frac{2\pi}{k_{e,n,m}} \left[\left(\frac{n}{a}\right)^2 + \left(\frac{m}{b}\right)^2 \right]^{-1/2} \\ &= \lambda_{h,n,m}\end{aligned}\tag{5.4}$$

Traditionally the rectangular guide is constructed with

$$b = \frac{a}{2}\tag{5.5}$$

This gives cutoff wavelengths for the next few modes as

$$\begin{aligned}\lambda_{h,2,0} &= a \\ \lambda_{h,0,1} &= a \\ \lambda_{e,1,1} &= \lambda_{h,1,1} = \frac{2a}{\sqrt{5}} = .89a\end{aligned}\tag{5.6}$$

For a given width a (and hence $\lambda_{h,1,0}$) the height b has been chosen as in (5.5) so that b is maximized without making $\lambda_{h,0,1}$ ($=2b$) any greater than $\lambda_{h,2,0}$. For this choice we have

$$\eta_f = \frac{\lambda_{h,1,0}}{\lambda_{h,2,0}} = \frac{\lambda_{h,1,0}}{\lambda_{h,0,1}} = 2\tag{5.7}$$

This gives the maximum relative bandwidth for the lowest order mode of a rectangular guide.

For this lowest order $H_{1,0}$ mode with (5.5) we have

$$\zeta_1 = \frac{\sqrt{3}}{2} = .866$$

$$\max_S |\nabla_t \psi_0(x,y)| = \max_C |\nabla_t \psi_0(x,y)| = \frac{\pi}{a}$$

$$\int_S |\nabla_t \psi_0(x,y)|^2 dS = b \left(\frac{\pi}{a}\right)^2 \int_0^a \sin^2\left(\frac{\pi x}{a}\right) dx$$

(5.8)

$$= \left(\frac{\pi}{a}\right)^2 \frac{ba}{2}$$

$$= \left(\frac{\pi}{a}\right)^2 \frac{a^2}{4}$$

$$\lambda_0 = 2a, \lambda_1 = a$$

$$n_1 = n_1' = \left[\frac{\sqrt{3}}{8}\right]^{1/2} = .465$$

This efficiency can serve as a standard for comparison to other shapes of waveguide cross section.

VI. Placing Perfectly Conducting Sheets in Waveguide Cross Section without Interfering with a Particular H Mode

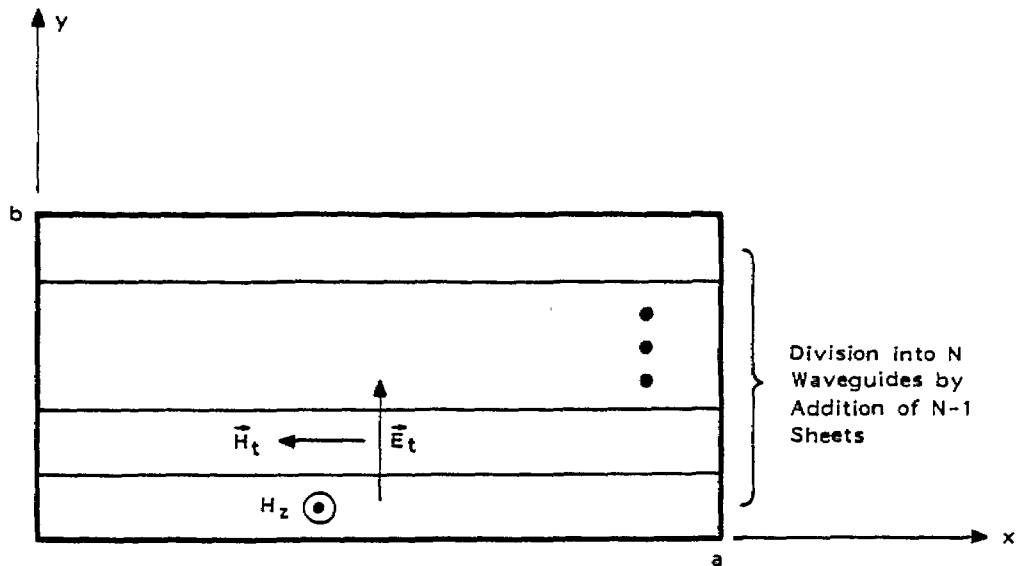
For various purposes one may wish to place conductors in a waveguide, or its extension as a horn. This is applicable to merging and dividing waveguides and for mechanical strengtheners as we shall see later.

Consider the modes as discussed in Section 2. Note that the E modes in (2.8) have both an E_z and an \vec{E}_t and that these have different distributions over S. One might place a conducting wire on some cross section (at a particular z) with this wire orthogonal to $\nabla_t \psi_{e,\beta}(x,y)$ for some β th mode of interest. However this wire cannot in the general case be extended in the z direction to form a conducting sheet without interfering with this same β th mode. To avoid this the sheet must be placed on a contour where $\psi_{e,\beta}$ is zero and this contour must also be orthogonal to $\nabla_t \psi_{e,\beta}$ (parallel to $\vec{i}_z \times \nabla_t \psi_{e,\beta}$) on S. There can be special cases of this (such as the $E_{0,m}$ rotationally symmetric modes of a circular waveguide) but this is not the usual case.

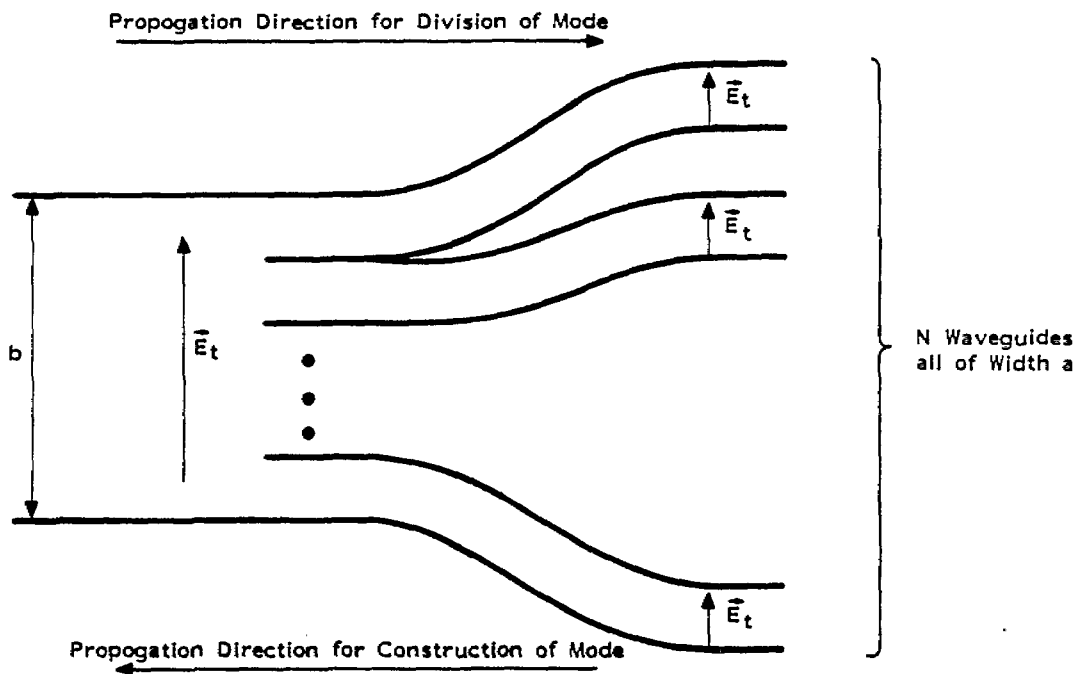
Now the H modes are a different matter. As in (2.4) there is no E_z . Thus we only need to consider \vec{E}_t . Then conducting sheets can be extended arbitrarily in the z direction. In the transverse sense these conductors can follow contours on S that are perpendicular to $\vec{i}_z \times \nabla_t \psi_{h,\beta}$, or equivalently parallel to $\nabla_t \psi_{h,\beta}$. Note that this direction can be expressed as a real-valued vector since the $\psi_{h,\beta}$ can be expressed as real valued functions on S. To see this note that with real-valued $k_{h,\beta}^2$ then (2.3) is satisfied by both $\psi_{h,\beta}$ and $\psi_{h,\beta}^*$. Adding the two Helmholtz equations shows that the Helmholtz equation is also satisfied by $\text{Re}[\psi_{h,\beta}]$ (and $\text{Im}[\psi_{h,\beta}]$ as well). So $\text{Re}[\psi_{h,\beta}]$ can be used as the mode (or any complex constant times $\psi_{h,\beta}$ for that matter).

Note also for the $\psi_{h,\beta}$ mode then \vec{H}_t is parallel to the conducting sheet as is H_z . This is another way of looking at the boundary conditions at the conducting sheet inserted in the waveguide. There can be no normal magnetic field at a perfect conductor.

As an example consider the rectangular guide as in Figure 6.1. In the lowest order $H_{1,0}$ mode the electric field is purely vertical and the magnetic field is purely horizontal (including the longitudinal part) as indicated in Figure 6.1A. The variations of the fields is independent of y with sine variation with respect to x for the transverse fields as in Figure 5.1. The longitudinal H_z has a cosine variation with respect to x (see (5.3)).



A. Addition of Conducting Sheets Orthogonal to Electric Field of $H_{1,0}$ Mode



B. Division of $H_{1,0}$ Mode or Construction of $H_{1,0}$ Modes from Matched $H_{1,0}$ Modes

Figure 6.1. Division of Rectangular Waveguide Operating in $H_{1,0}$ Mode

In Figure 6.1A $N-1$ conducting sheets are added on planes of constant y within the waveguide. This gives N waveguides, the heights of which sum to b , and the widths of which are all a . Now as in Figure 6.1B let these sheets begin on some cross section to divide the one waveguide on the left into N waveguides on the right. Then one can make each dividing sheet become two sheets which are gradually separated so that N separated waveguides are formed.

If the $H_{1,0}$ mode is propagating from the left, it divides into the $H_{1,0}$ modes of the N waveguides, the power in each guide being proportional to its height. If desired each of these N guides can be gradually expanded to the usual height of $a/2$ for lower losses. This type of matched power divider might have various applications, such as to feed an array of N radiating horns.

Conversely, one can have N waves propagating from the right in the $H_{1,0}$ modes of the N waveguides. Provided the fields arrive at the cross section where the N guides become one and the fields match between adjacent guides then one $H_{1,0}$ mode propagates out to the left. This requires that not only the amplitudes, but phases as well match at this cross section. For simplicity one might have the heights of each guide on the right as b/N with equal powers in each of these guides. Then the important issue is to have the phases of the N waves all match at the interface to the guide to the left. If the N sources driving the waves in the N guides are all of the same frequency then phases need to be adjusted in the sources and/or the waveguide delays to establish the matching conditions.

Note that the N guides on the right are in general curved different amounts so that the delays in the different guides are perturbed differently (as compared to a straight waveguide). Symmetry can be used to provide some exception to this. For example for $N=2$ one can have a symmetry plane (one guide being the mirror image of the other) as the two guides are bent away from each other (E plane bends). The right guides in Figure 6.1B can have one bend into and the other bend out of the page (H plane bends). This is an example of rotation symmetry about the axis ($x = a/2, y = b/2$) of the left guide. Combinations of various bends and twists of the two guides can be made

subject to the symmetry that rotation by π around the object leaves the geometry unchanged. Note that for $b = a/2$ the two waveguides each have width a and height $a/4$.

Using this 2-symmetrical a by $a/4$ guide system one could connect the guides to two sources with identical phases and have the two signals combine without reflection into the single a by $a/2$ guide. Such might be two ports on a single magnetron.

This concept can be extended by dividing a locally straight section in each a by $a/4$ guide into two a by $a/8$ guides. Then proceeding with each pair as above we have four a by $a/8$ guides which can be used to combine four signals without reflection into the single a by $a/2$ guide. Such might be four ports on a single magnetron.

VII. Vacuum Interface at Horn Exit

Another application of these non-interfering sheets in a waveguide cross section is as a grating to support a dielectric sheet serving as a gas barrier. Suppose for simplicity we consider a rectangular or pyramidal horn as in Figure 7.1. The horn might be considered as a conical waveguide or a gradually expanding rectangular waveguide. Care should be taken that at the mouth (aperture or exit) of the horn the fields are like the $H_{1,0}$ mode, specifically that the electric field is at least approximately perpendicular to the metal slats (grating) placed across the mouth of the horn.

One purpose of the horn is to expand the power in the waveguide so that the electric field is considerably reduced at the aperture. If the waveguide is operated under high-vacuum conditions it can propagate very large electric fields. In order to bring the power out of the waveguide the fields need to be reduced if the dielectric medium is air or some high dielectric strength gas (such as SF_6 at one atmosphere). Choosing the aperture dimensions to avoid breakdown one transitions these back to the waveguide via the evacuated horn.

Note that at the aperture the wave is ideally to pass through the grating with no disturbance. Of course there will in general be some perturbation due to the grating. It may be desirable to avoid resonant currents on the slats. This can be done by making the slat length an odd number of quarter wavelengths, or by addition of appropriate impedance loading.

Variations on the design of the horn aperture are possible as indicated in Figure 7.2. Begin with a flat dielectric sheet in Figure 7.2A. Note the metal slats supporting the gas pressure through the dielectric sheet. In Figure 7.2B one might replace the flat dielectric sheet by some sort of ridged sheet, both for pressure reasons and dielectric-strength reasons. Figure 7.2C shows an example in which the grating is not against a single flat surface, but pushes the center of the aperture out so that the electric field is not parallel to the dielectric sheet.

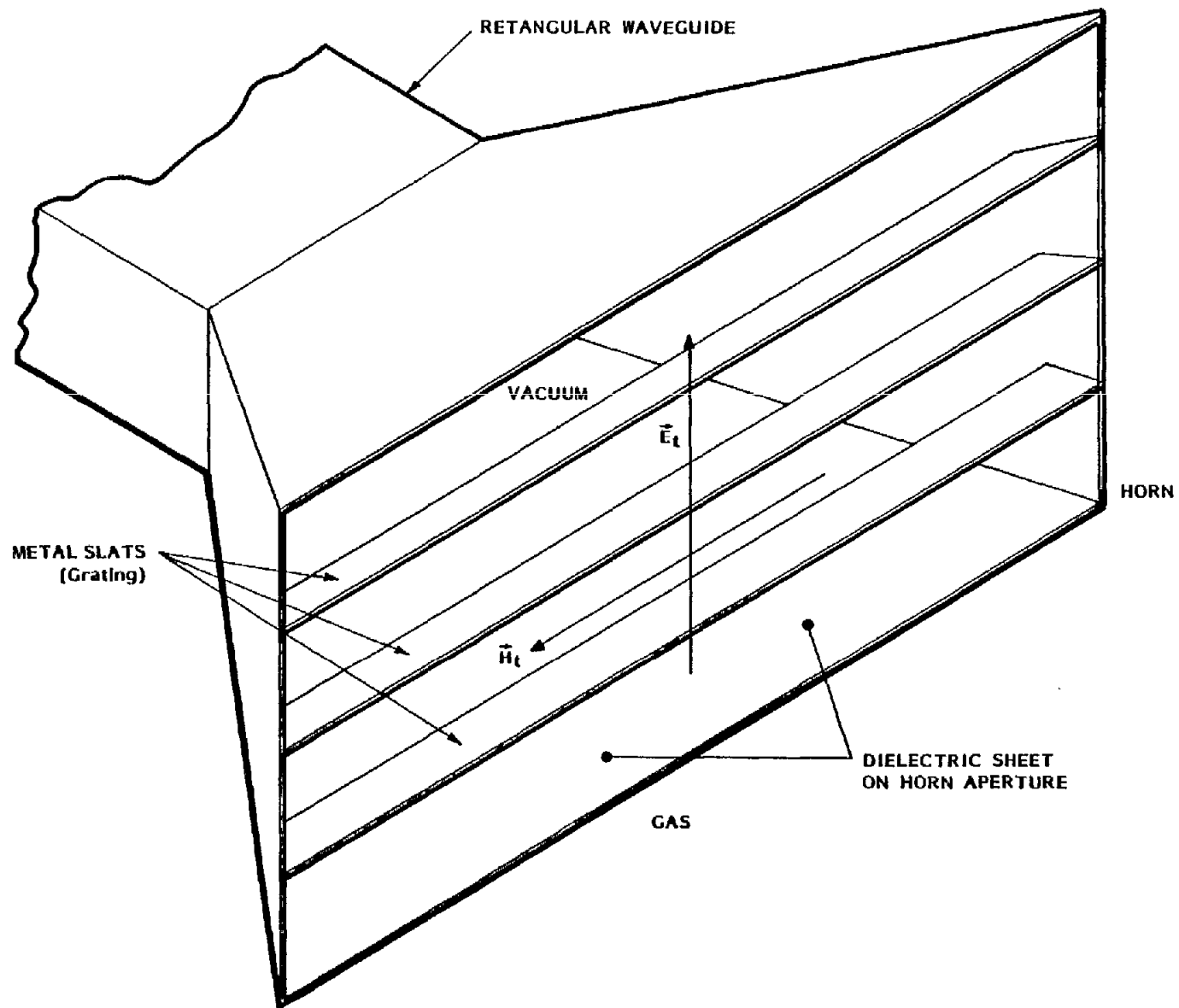


Figure 7-1. Dielectric Sheet and Metal Grating at Horn Aperture

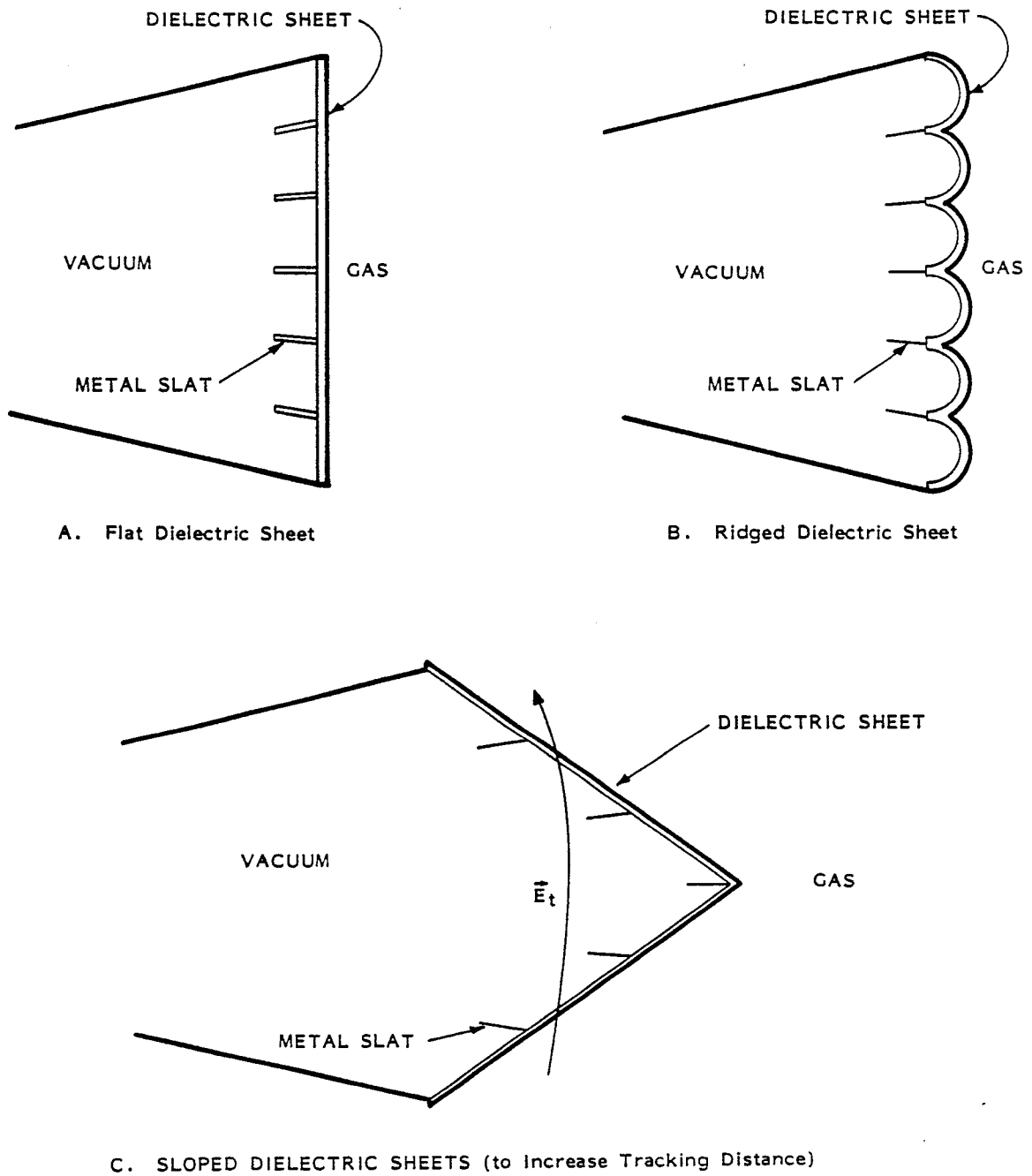


Figure 7.2. Vacuum/Gas Interfaces at Horn Aperture

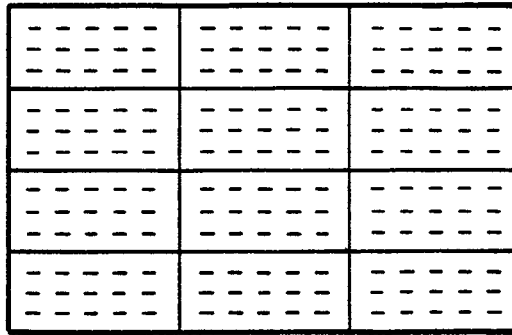
VIII. Arrays of Horns

For various reasons one may have the electromagnetic wave to be released into the air (or other gas medium) present on more than one waveguide. Then one may transition the M waveguides via M horns with the aperture surfaces all on a common desired surface such as a plane or sphere. The M signals are assumed to be all in phase with respect to this surface.

There are various ways that one may arrange horns to form a two-dimensional array. For simplicity approximating the array surface as a plane, the array may be considered as a periodic structure, a few examples of which are illustrated in Figure 8.1. Using rectangular horns (a by $a/2$) we have the in-line and staggered arrays as in Figure 8.1A and Figure 8.1B. Note the presence of the gratings with parallel slats. A limitation of such an array is that the $H_{1,0}$ mode is not uniform across each horn, but has \vec{E}_t going to zero at the "side" walls (walls parallel to the E field direction). This means that the electric field distribution over the array surface is (undesirably) nonuniform.

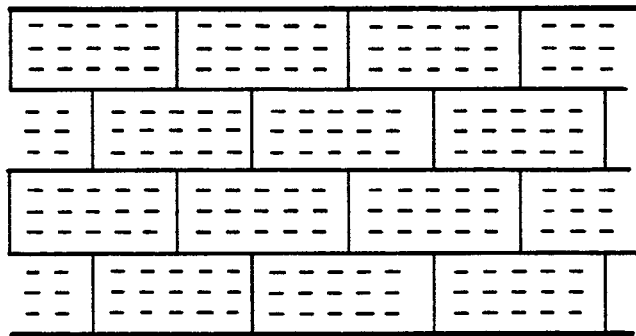
An alternate approach is illustrated in Figure 8.1C. The rectangular waveguides are transitioned to rhombic (diamond shaped) waveguides with about a 2 to 1 width to height ratio so that the corresponding dominant H mode is effectively excited. These waveguides are then expanded as conical horns with rhombic cross sections. These horns fill the array plane as in Figure 8.1C. Noting the symmetry of these diamonds at least one conducting slat can be placed across the center of each and be perpendicular to \vec{E}_t . However, off the symmetry plane the slats are in general not flat for the lowest order H mode. In this geometry the distribution of \vec{E}_t is such that it is perpendicular to the diamond boundaries. This gives a smooth transition from one horn to the next. While the rectangular $H_{1,0}$ distribution has zero electric field along each "side" boundary, the corresponding diamond distribution crowds this null into the "corners".

In general there are various details for optimizing horn arrays. The horn shape and arrangement as above is but one question. Tapering the distribution across the array (say by variation in the horn design, especially near the edges of the array) is another interesting question. Perhaps other horn shapes for arrays need to be considered.

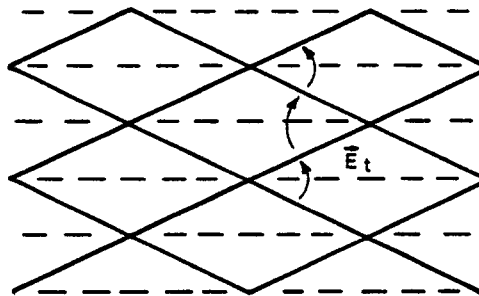


GRATING SLATS

A. In-Line Rectangular Horns



B. Staggered Rectangular Horns



C. Rhombic Horns

Figure 8.1. Horn Arrays with Aperture Gratings

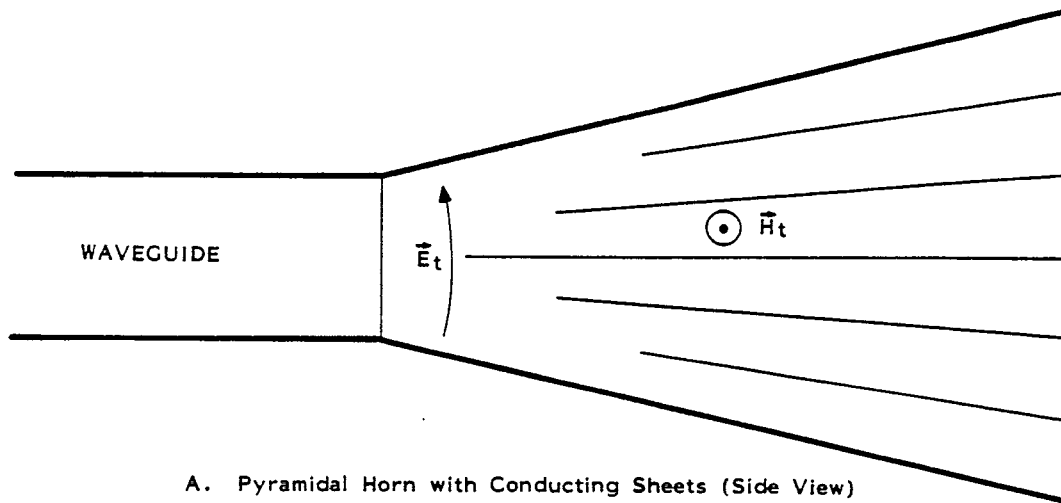
IX. Lenses in Horns

In designing the horn or array of horns that launches a wave one may be concerned with controlling the phase distribution on the horn aperture(s). This depends on the type of wave (e.g. planar or spherical) that one wishes to synthesize, and on the uncorrected phase distributions in the horn aperture(s). One can insert some kind of lens in the horn to adjust the phase distribution in the horn aperture toward some more desirable distribution. Reflections from this lens should also be minimized since these would reduce the power radiated.

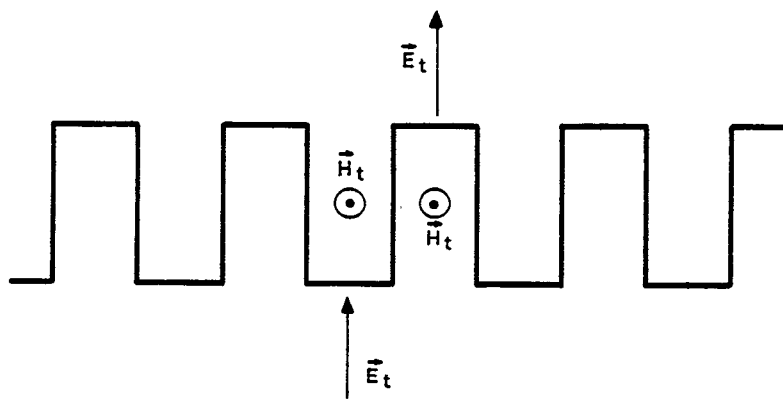
One interesting kind of lens involves modifications to the grating design in Section 7. As indicated in Figure 9.1A extend the grating slats back into the throat of a pyramidal horn. Note that these sheets, if extended, would have a common apex, the same apex as the pyramidal horn. As discussed before in the context of the grating slats these sheets (assumed perfectly conducting) do not interfere with the field distribution of the $H_{1,0}$ mode.

Now modify these conducting sheets so as to create a slow wave structure [4] as in Figure 9.1B. The magnetic field \vec{H}_c can penetrate into the grooves (including on both sides if desired). As the horn expands so that there are many wavelengths in the H direction (between the side walls), one can think of the wave propagating between two sheets as locally a TEM plane wave. Corrugating the sheets then can be approximately analyzed as a two-dimensional problem [4]. The top and bottom surfaces of the horn (E plane walls) can also be corrugated as in a typical corrugated pyramidal horn [5].

By varying the corrugations (depth, width, and/or spacing) along the length and width of the sheets various propagation speeds (phase speeds) can be achieved. Thereby the phase at the horn aperture can be controlled to some extent. Note that one may wish to vary the corrugation parameters slowly so as to not introduce significant reflections. Furthermore, the conducting sheets need to be close enough together (say less than a half wavelength at the horn aperture) to avoid introduction of higher order modes between the sheets by the effective impedance boundary condition of the corrugations.



A. Pyramidal Horn with Conducting Sheets (Side View)



B. Corrugated Conducting Sheets

Figure 9.1. Corrugated Conducting Sheets in Horn Making Slow-Wave Structure for Lens

References

1. C.E. Baum, Maximization of Electromagnetic Response at a Distance, Sensor and Simulation Note 312, October 1988.
2. F.E. Borghis and C.H. Papas, Electromagnetic Waveguides and Resonators, in S. Flugge/Marburg (ed.), Encyclopedia of Physics, vol. 16, Springer, 1958.
3. R.E. Collin, Field Theory of Guided Waves, McGraw Hill, 1960.
4. R.E. Collin, Foundations for Microwave Engineering, McGraw Hill, 1966.
5. C.A. Balanis, Horn Antennas, in Y.T. Lo and S.W. Lee (eds.), Antenna Handbook, Van Nostrand Reinhold, 1988.